



## SiGe based grating light valves: A leap towards monolithic integration of MOEMS

S. Rudra<sup>a,\*</sup>, J. Roels<sup>a</sup>, G. Bryce<sup>b</sup>, L. Haspelslagh<sup>b</sup>, A. Witvrouw<sup>b</sup>, D. Van Thourhout<sup>a</sup>

<sup>a</sup> Photonics Research Group, INTEC Department, Ghent University – IMEC, Gent, Belgium

<sup>b</sup> IMEC, Kapeldreef 75, Leuven 3001, Belgium

### ARTICLE INFO

#### Article history:

Received 22 September 2009

Received in revised form 24 November 2009

Accepted 6 December 2009

Available online 22 December 2009

#### Keywords:

Optical MEMS

SiGe

Diffraction gratings

### ABSTRACT

The Grating Light Valve (GLV) is a microelectromechanical reflection grating. It operates on the principle of controlled diffraction of incident light due to electrostatic deflection of microbeams, thus producing bright and dark pixels in a display system. This unique approach offers significant advantages compared to other display systems in terms of speed, high optical efficiency, accuracy and ease of manufacturing. At the same time monolithic integration of MEMS on top of CMOS is getting more popular because CMOS-integrated MEMS exhibit less parasitics and have a reduced assembly and packaging cost over hybrid approaches. The relatively low deposition temperature ( $\sim 450^\circ\text{C}$ ) of poly-SiGe compared to poly-Si ( $\sim 800^\circ\text{C}$ ) makes poly-SiGe suitable for back end processing. Hence, in this work we report the fabrication and functioning of CVD poly-SiGe GLVs in terms of their response to the amplitude and frequency of the applied actuation voltage.

© 2009 Elsevier B.V. All rights reserved.

### 1. Introduction

Grating Light Valve [1,2] (GLV) display pixels are reflection type diffraction gratings. They consist of parallel microbeams moving up and down in response to an electric field forming a square well grating with changing phase as shown in Fig 1a. In the non-actuated state, coplanar beams behave like a mirror giving a specular reflection in the 0th order. The pixel is then in the OFF state, with no light diffracted to the  $\pm 1$ st order. After actuation, the alternate movable beams are deflected downwards and the grating starts diffracting, which turns the pixel ON. At a deflection of  $\lambda/4$ , the amount of light diffracted to the  $\pm 1$ st order reaches its maximum. Display systems made from this technology provide a huge improvement in contrast ratio, high resolution and brightness [1,2] over other display systems. Recently it was reported that GLV based modulators can also be used in time of flight applications [3].

The GLV microbeams we use are clamped–clamped (fixed–fixed) beams suspended in air over a substrate with the help of anchors on two far ends. They can be described by a spring capacitor model. The electrostatic force associated with the constant voltage drive mode is nonlinear and gives rise to the well known phenomenon of pull-in [4,5]. The electrostatically actuated beams collapse on the ground plane once the highest deflection exceeds approximately one-third of the airgap ( $d_0$ ). Hence in a GLV structure, the airgap between beams and the underlying ground substrate is designed in such a manner that  $d_0/3 > \lambda/4$ . The actuation voltage is therefore always maintained well below the pull-in voltage, saving it from deterioration.

Another important issue is the integration of micro electro mechanical systems (MEMS) with CMOS [6]. In hybrid integration, separate chips for MEMS and IC are used which results in performance limiting parasitics because of the interconnections between them. These parasitics occur mainly from the size of the bondpads and from the long bonding wires. Comparatively, post processing of MEMS monolithically on top of CMOS can lead to increased functionality, performance, reliability and a higher miniaturization. However, post processing limits the thermal budget for the MEMS processing. Poly-SiGe provides the necessary mechanical properties and reliability required for MEMS applications at a significant lower temperature compared to poly-Si (i.e. deposition temperatures of  $\sim 450^\circ\text{C}$  instead of  $\sim 800^\circ\text{C}$ ). Hence, recently poly-SiGe has attained serious attention in post processing MEMS above CMOS [7]. Monolithically integrated micro-mirror arrays [8,9] are already reported. They can be used in applications such as video projection, adaptive optics, mask writers, etc.

The purpose of this work is to show the functionality of poly-SiGe GLVs with different beam lengths. A clear length dependent change in resonance frequency of the devices is observed, as shown below. We will demonstrate that high switching speeds can be obtained and that a reasonable voltage dependent change in diffraction efficiency can be produced.

### 2. Fabrication and appearance of GLVs

The SiGe structural layer used in these devices is 300 nm thick. The CVD deposited structural SiGe layer was grown with a  $\text{SiH}_4:\text{GeH}_4$  flow ratio of 0.9:1 and 69 sccm  $\text{B}_2\text{H}_6$  at a chuck temperature of  $460^\circ\text{C}$  ( $\sim$ wafer temperature of  $450^\circ\text{C}$ ). After roughness

\* Corresponding author.

E-mail address: [sukumar.rudra@intec.ugent.be](mailto:sukumar.rudra@intec.ugent.be) (S. Rudra).

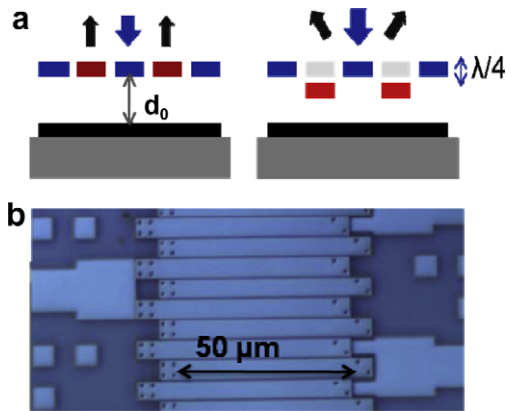


Fig. 1. (a) Schematic representation of the working principle of a grating light valve. (b) Microscope view of GLV pixels consisting of two fixed and two movable beams.

reduction of the SiGe layer by CMP, extra layers consisting of 5 nm SiC and 30 nm AlCu were added. The AlCu layer is sputter-deposited at room temperature for high reflectivity and the SiC layer acts as a barrier layer to prevent diffusion between SiGe and Al. Finally the samples were released in vapor HF. Rutherford backscattering spectroscopy (RBS) data revealed a Ge concentration of about 78% in the SiGe layer [10]. Fig. 1b shows the pixel configuration of the GLVs and the connection towards bondpads. A total of 16 pixels constitute a single GLV device. Three different beam lengths of 50  $\mu\text{m}$ , 100  $\mu\text{m}$  and 200  $\mu\text{m}$  were fabricated with a pitch of 4.8  $\mu\text{m}$  and a fill factor of 93%. The airgap between the beams and the substrate was maintained at 0.6  $\mu\text{m}$ , allowing GLV operation over the whole visible spectrum.

### 3. Experimental characterization system

Fig. 2 shows the experimental set-up used for characterization of the GLVs. The two convex lenses in the front act as a collimator. The cylindrical lens focuses the light as a horizontal line with uniform intensity on the center of the microbeams. The beamsplitter helps in separating the incoming and outgoing light. A photodiode in series with an electrical spectrum analyzer gives the intensity of the diffracted light as a function of amplitude and frequency of the applied actuation voltage.

### 4. Results and discussion

To ensure a safe operation, the pull-in voltage of different GLVs with varying beam lengths was estimated. COMSOL Multiphysics [11] (based on finite element method analysis) was used to calcu-

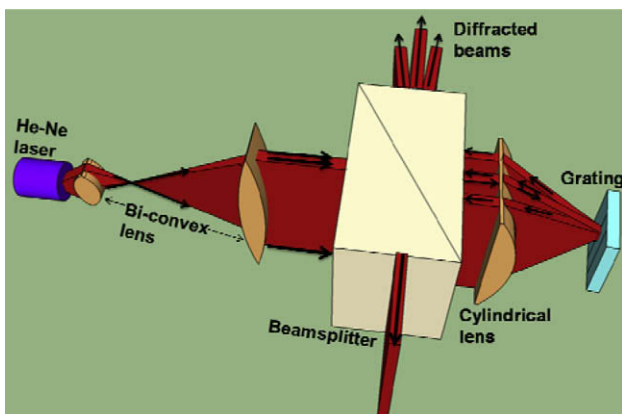


Fig. 2. GLV characterization set-up.

late the pull-in voltage of the devices using a fixed-fixed beam model. As can be seen from Fig. 3 the pull-in voltage for 50  $\mu\text{m}$ , 100  $\mu\text{m}$  and 200  $\mu\text{m}$  beams vary widely, which can be verified easily using an analytical spring capacitor model as reported in literature [4,12]. A Young's modulus of 143 GPa and a density of 4725  $\text{kg}/\text{m}^3$  was assumed for the simulation and the theoretical calculations [11].

Once the safe operating range was determined, the GLV devices were thoroughly characterized. Proper understanding of the dynamic characteristics of electrostatically actuated microbeams is of utmost importance for the MEMS devices. GLV microbeams can be well described by a forced, damped, harmonic oscillator for which the response time decreases with increasing resonant frequency and damping coefficient. We measured the resonant frequency to estimate the switching speed of the devices. The change in optical intensity under DC actuation was also monitored to determine the contrast of the present device. To find the frequency response of the devices, a small sinusoidal signal ( $V_{AC}$ ) was used in combination with a larger DC voltage ( $V_{DC}$ ) to modulate the beams around a stable deflected distance. This creates a force with two different harmonics of the applied signal but the 1st harmonic dominates largely over the 2nd one because of the small amplitude of the sinusoidal signal:

$$F \propto [V_{DC} + V_{AC} \cos \omega t]^2 \\ \rightarrow \left[ \left( V_{DC}^2 + \frac{V_{AC}^2}{2} \right) + 2V_{DC}V_{AC} \cos \omega t + \frac{V_{AC}^2}{2} \cos 2\omega t \right]$$

The small signal frequency response of the devices is shown in Fig. 4 where a clear increase in resonance frequency with decreasing length of microbeams can be observed. Using a spring capacitor model theoretical [13,14] resonance frequencies of 703 kHz, 175 kHz and 44 kHz were found respectively for the 50, 100 and 200  $\mu\text{m}$  beams which is in relative agreement with the experimentally determined values of 920 kHz, 255 kHz and 124 kHz. The reason behind the deviation between experimental and theoretical values may be related to: (1) the application of a relatively high DC voltage causes initial bending and gives rise to a tensile stress inside the beams which was not taken into account in the theoret-

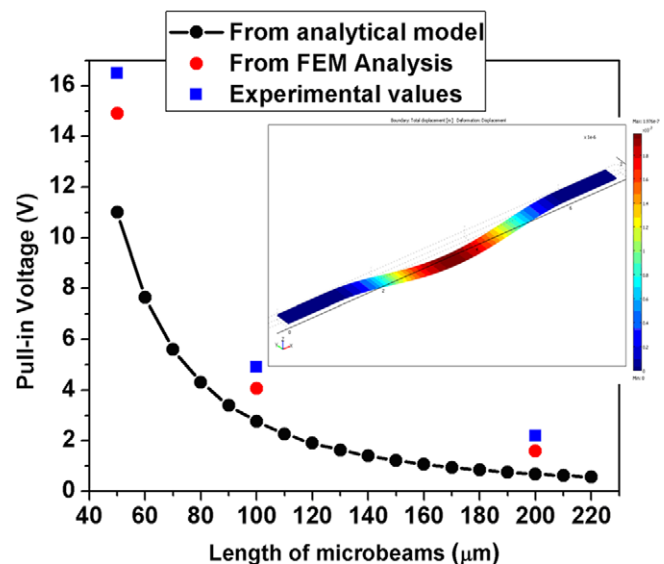


Fig. 3. Comparison of pull-in voltage values with change in beam length as found from finite element analysis using COMSOL, an analytical model [12] and experiments. The inset shows a typical COMSOL simulation of bending of a 50  $\mu\text{m}$  long and 4.5  $\mu\text{m}$  wide fixed-fixed electrostatically actuated SiGe beam with an airgap of 0.6  $\mu\text{m}$ .

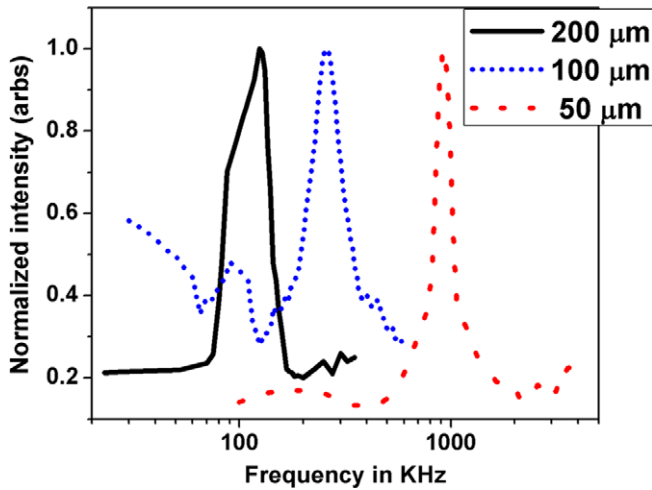


Fig. 4. Small signal frequency response of GLVs with 50, 100 and 200  $\mu\text{m}$  long beams.

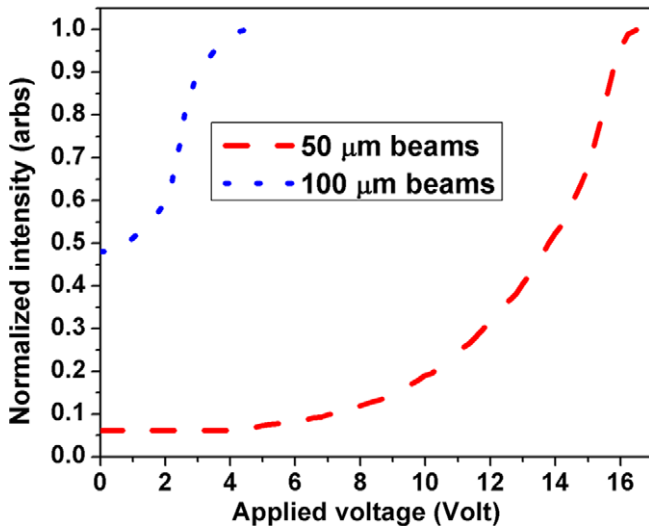


Fig. 5. Change in 1st order diffraction intensity with actuation voltage for two different GLVs.

ical calculations, or (2) an uncertainty in the estimated Young's Modulus and density of the poly-SiGe material. We also determined experimental Q factors of 1.6, 3.2 and 5.2 respectively for the 200, 100 and 50  $\mu\text{m}$  beams. These relatively small Q's can be attributed to the air damping in open atmosphere.

The response of the GLVs to a DC voltage is shown in Fig. 5. A clear change in the intensity of the 1st order diffracted light with increasing actuation voltage can be observed. Whereas for the 100  $\mu\text{m}$  beams the change is less prominent and the dark state intensity is high, the 50  $\mu\text{m}$  beams show an excellent overall behavior. This might be related to the intrinsic stress in the structural SiGe/SiC/Al stack. This stress could not be measured accurately due to stress changes in the underlying Si-oxide layer during the deposition of the structural layer. However, as the 50  $\mu\text{m}$  beams are flat and the 100  $\mu\text{m}$  and longer beams seem slightly buckled, the intrinsic stress is probably compressive. It is expected that the deficient behavior of the long beams can be improved by introducing a tensile stress in the beams.

## 5. Conclusion

We have demonstrated the operation of a poly-SiGe based GLV for the very first time. GLVs of 50  $\mu\text{m}$  showed a good tuning behavior with a resonance frequency of 920 kHz. Our next goal is to implement a residual tensile stress in the microbeams which will improve the switching speed and the dark state intensity level.

## References

- [1] D. Bloom, The grating light valve: revolutionizing display technology, in: SPIE Proc., Projection Displays III Symposium, vol. 3013, 1997, pp. 165–171.
- [2] Jahja Trisnadi et al., Photonics West, Micromachining and Microfabrication symposium, Paper 5348-05, 2004.
- [3] J. Roels et al., Photonics Technol. Lett. 20 (2008) 1827.
- [4] G.M. Rebeiz, R.F. MEMS, Theory Design and Technology, John Wiley and Sons, 2003, pp. 21–31.
- [5] D. Peroulis et al., IEEE Trans. Microwave Theory Techniques 51 (2003) 259–270.
- [6] R. Jablonski, M. Turkowski, R. Szewczyk, Recent Advances in Mechatronics, Springer, Berlin, Heidelberg, 2007, pp. 521–525.
- [7] A. Witvrouw, Scripta Mater. 59 (2008) 945–949.
- [8] M. Gromova et al., Proc. IEEE MEMS (2007) 759–762.
- [9] L. Haspeslagh, J. De Coster, et al., Proc. IEDM 2008 (2008) 655–658.
- [10] G. Bryce et al., Proc. ECS 2008, ECS Transactions 16 (10) (2008) 353–364.
- [11] M. Uncuer et al., in: Proc. COMSOL Conference 2007, p. 439.
- [12] S. Chowdhury et al., J. Micromech. Syst. 15 (2005) 756–763.
- [13] W.T. Thomson, Theory of Vibration with Applications, Prentice Hall, Englewood Cliffs, NJ, 1981.
- [14] K. Wang et al., J. Microelectromech. Syst. 9 (2000) 347–360.